Struct Chem (2010) 21:787–793
DOI 10.1007/s11224-010-9612-z

ORIGINAL RESEARCH

Gas-phase conformations and exciton couplings in 5,6,11,12-tetrahydrodibenzo[*a*,*e*]cyclooctene

Abdulhamid Hamza

Received: 30 November 2009 / Accepted: 12 April 2010 / Published online: 23 April 2010

Abstract The conformations and exciton couplings in 5,6,11,12-tetrahydrodibenzo[*a*,*e*]cyclooctene (THDC) have been studied using resonance-enhanced two-photon ionization spectroscopy in a supersonic jet expansion. It has been estimated from the spectral analysis that 90% of THDC exists in the twist-boat (TB) conformation; the chair (C) conformer constitutes the remaining 10%. Most of the vibronic activity in the spectrum of THDC is associated with the symmetric flapping of the aromatic rings of the TB conformer. The observed S_1/S_2 exciton splitting of the TB conformer is 100 cm^{-1}. The S_1/S_2 transition of the C conformer is found to be forbidden. The exciton splittings of the C and TB conformers were estimated by the spectral analysis of two deuterated isotopomers of THDC. The estimated exciton splittings of the C and TB conformers are 14.7 and 101.9 cm^{-1}, respectively. The supramolecular model of bichromophores with identical chromophores at the CIS/6-31+G(d)//HF/6-31+G(d) level of theory predicted electronic coupling energies that are very close to the experimental exciton coupling energies.

Keywords
5,6,11,12-Tetrahydrodibenzo[*a*,*e*]cyclooctene · Conformation · Exciton coupling · Spectroscopy · Ab initio calculations

Introduction

The conformations of 5,6,11,12-tetrahydrodibenzo[*a*,*e*]cyclooctene (THDC), also known as [2.2]-orthocyclophane, have been extensively investigated by X-ray and NMR techniques [1–3]. Previous theoretical studies of THDC were limited to molecular mechanics and density functional theory (DFT) calculations [3, 4]. The calculations predicted three stable ground state conformers. The structures of the three stable conformers are displayed in Fig. 1. The twist-boat (TB) and chair (C) conformers have been observed in solution using NMR techniques [2, 3]. X-ray studies show that only the C conformer is present in the crystal [1]. The gas-phase conformational analysis of THDC which can be readily compared with the results of theoretical computations of the isolated THDC conformations has not yet been reported in the literature.

The photophysical properties of THDC have been studied by Longworth and Bovey [5]. THDC absorbs and fluoresces in the same spectral region as 1,2-diphenylethane and other alkylbenzenes. However, the fluorescence of THDC is unstructured, and has a small quantum yield. The authors therefore, concluded that the interaction of the two aromatic rings of THDC in the excited state is weak, and the molecule undergoes geometrical changes upon electronic excitation [5]. Hence, THDC can be treated as a covalently bonded dimer of *o*-xylene. The scope of the exciton theory is to relate the excited states of dimers to those of the constituting monomers. The excitation energy of dimers (bichromophoric molecules) that incorporate two identical chromophores is shared by the chromophores via exciton coupling. The strength of the exciton coupling is determined by the electronic coupling energy, V [6–9]. The observed exciton splitting, $2V_{vv}$, of the vibronic bands is composed of the purely electronic and vibrational components.

A. Hamza (✉)
Petroleum Chemistry and Engineering Program, School of Arts and Sciences, American University of Nigeria, PMB 2250, Yola, Nigeria
e-mail: abdulhamid.hamza@aun.edu.ng; abbamid@yahoo.com

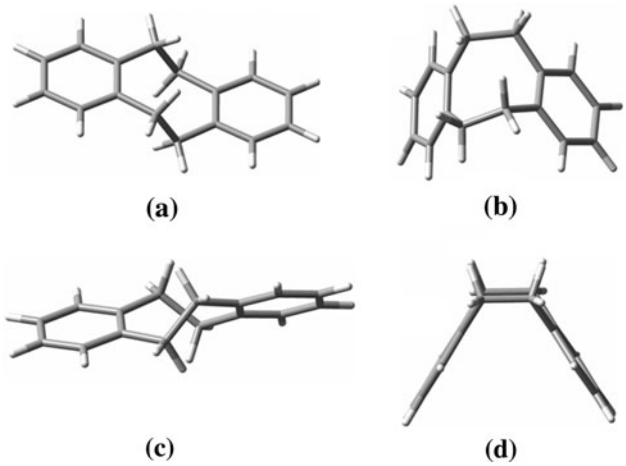

Fig. 1 Optimized ground state structures of the **a** chair (C), **b** twist-boat (TB), **c** twist (T), and **d** boat (B) conformations of THDC. The boat conformation corresponds to a transition state between two equivalent TB conformers

The vibrational component is determined by the Franck–Condon factor, FC_{vv}, of the vibronic transition [9]. The electronic component, V, is composed of terms describing the through-space (Coulombic and exchange) and through-bond mediated interactions of the chromophores [6–9]. The electronic component, V, can be estimated from the experimental data by dividing V_{vv} with FC_{vv} [9].

In this work, THDC and its two selectively deuterated isotopomers have been synthesized. The structures of the synthesized isotopomers are shown in Fig. 2. The gas-phase electronic spectra of the THDC isotopomers have been recorded in a supersonic jet. Analysis of the experimental data in combination with ab initio electronic structure calculations provides information about the conformational preferences of THDC in the gas phase and the S_1/S_2 exciton coupling energies of THDC conformers.

Experimental and computational methods

A modified procedure of Boudjouk et al. [10] was used for the synthesis of THDC-d_0 in about 80% yield. The procedure involves sonication of α,α′-dibromooxylene (7.6 mmol) and lithium granules (30 mmol) in 15 mL of THF under argon atmosphere. After 3 h of sonication at room temperature, the reaction mixture was cooled to ca. 0 °C. 20 mL of cold water was then slowly added to destroy the remaining lithium granules. The organic layer was extracted with diethylether. The product was purified by column chromatography on silica gel (petroleum ether) to give pure THDC-d_0. A statistical mixture of THDC-d_0, THDC-d_4, and THDC-d_8 was synthesized by coupling of α,α′-dibromooxylene-d_4 (4 mmol) and α,α′-dibromoxylene-d_0 (4 mmol) following the same procedure as for THDC-d_0. α,α-Dibromooxylene-d_4 was synthesized in two steps. A mixture of phthalic acid-d_4 (5.8 mmol) and $LiAlH_4$ (6.5 mmol) in 20 mL of THF was refluxed for 15 h to yield α,α′-benzenedimethanol-d_4. Reaction of α,α′-benzenedimethanol-d_4 (5 mmol) with 1.5 equivalent of PBr_3 in 20 mL of dichloromethane at 20 °C for 2 h yielded α,α′-dibromooxylene-d_4. The identity of the synthesized compounds was confirmed by GC/MS analysis.

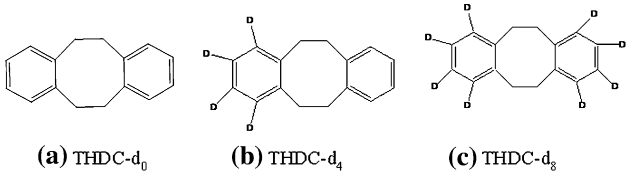

(a) THDC-d_0 **(b)** THDC-d_4 **(c)** THDC-d_8

Fig. 2 Investigated isotopomers of THDC

The supersonic jet spectrometer used in this work has been described in details elsewhere [11]. Briefly, the spectrometer is composed of two differentially pumped expansion and ionization chambers. The sample of THDC isotopomers is heated to 140 °C, and seeded in a carrier gas (helium or neon) at a backing pressure of 2–3 atm. The free jet in the expansion chamber is skimmed, and the resulting molecular beam in the ionization chamber is perpendicularly crossed by a frequency doubled, Nd:YAG pumped dye laser beam. Molecular ions are formed by sequential absorption of resonant and ionizing laser photons. The molecular ions are then detected and mass analyzed using a time of flight mass spectrometer. Resonance-enhanced two-photon ionization (R2PI) spectra are measured using a boxcar integrator interfaced with a personal computer.

Ground state geometry optimizations were carried out at the Hartree–Fock (HF), the density functional theory (DFT) with the B3LYP functional, and the second-order Møller–Plesset perturbation (MP2) levels of theory. Harmonic frequency calculations were done at the HF and DFT levels using the HF and DFT optimized geometries, respectively. Configuration interaction singles (CIS) method was used for computing vertical excitation energies using the HF optimized S_0 geometries. The computations were performed using the 6-31+G(d) basis set. All calculations were performed using Gaussian 03 suite of programs [12].

Results and discussion

Ab initio calculations

The calculated S_0 relative energies and molecular symmetries of the three stable conformers of THDC are presented in Table 1. The MP2 calculations predicted more stable TB conformer. Whereas, the C conformer is predicted to be the most stable at the HF and DFT levels of

Table 1 Relative energies (in kJ/mol) and symmetries of the three stable conformers of THDC at various levels of theory with 6-31G+(d) basis set

Conformer	Symmetry	HF	DFT	MP2	MP2//HF
TB	C_2	0	0	0	0
C	C_{2h}	−3.52	−3.76	11.76	5.84
T	D_2	12.73	10.89	27.91	22.33

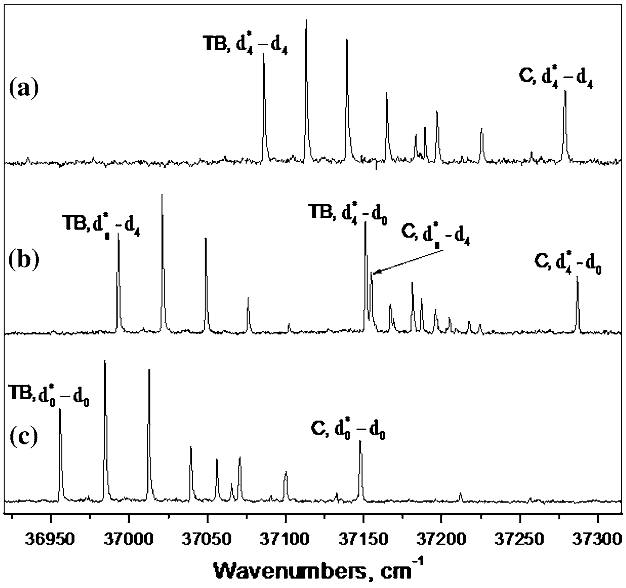

Fig. 3 R2PI spectra of **a** THDC-d_8, **b** THDC-d_4, and **c** THDC-d_0. Two localized electronic origins of each conformer appear in the spectrum of THDC-d_4

theory. The difference between the MP2 and HF/DFT results can be attributed to the fact that the MP2 method better accounts for the non-bonded intramolecular dispersive interactions between the π electron clouds of the aromatic rings [13]. These interactions are particularly important in the TB conformer, where the aromatic rings are closer and partially overlapping. However, the MP2 method often overestimates conjugation [14], which might lead to overestimation of the relative stability of the TB conformer in which dispersive interactions between the π electron clouds are possible. Smith et al. [15] reported that better relative energies of the various configurations of the benzene dimer (where dispersive interactions play an important role in determining the relative stability of the various configurations of the dimer) are obtained by performing single point MP2 energy calculations on HF optimized geometries. The results of this work also reveal that the single point MP2 relative energies on HF optimized geometries of THDC conformers are in excellent agreement with the experimental relative conformational energies (vide infra).

The T conformer is predicted to be the highest in energy by the HF, DFT, and MP2 methods. Therefore, the T conformer may not be observed in the supersonic jet experiments owing to negligible Boltzmann factors at the experimental temperature of 140 °C. The B conformation corresponds to a transition state between two equivalent TB conformers, as the single imaginary frequency (−109 and −123 cm^{-1} at the DFT and HF levels, respectively) that is associated with torsions about the central $C_{sp^3} - C_{sp^3}$ a bond implies.

R2PI spectra

The R2PI spectra of THDC-d_0, THDC-d_4, and THDC-d_8 are presented in Fig. 3. The first band in the spectrum of THDC-d_0 appears at 36956.3 cm^{-1}; scanning to the red of this peak did not reveal additional spectral features. Therefore, the band at 36956.3 cm^{-1} can be assigned to the electronic origin of one of the THDC conformers. Generally, a peak in any vibrationally resolved electronic spectrum may be assign to vibrationless electronic origins (0_0^0) of conformers or vibrational modes. It is well known that isotopic substitution has much higher effect on the frequencies of vibrational transitions than on the relative 0_0^0 transition energies of conformers [16]. Therefore, vibrationless electronic origins of conformers can be readily distinguished from vibronic peaks based on the observed isotope effects. Herein, the isotope effect on the relative frequencies of the observed peaks in the R2PI spectrum of THDC has been studied in order to determine the number of THDC conformers that are present in the gas phase and assign their vibronic transitions.

The spectrum of the symmetrically deuterated THDC-d_8, shown in Fig. 3a is qualitatively similar to that of THDC-d_0 (Fig. 3c), as both THDC-d_0 and THDC-d_8 have the same symmetry. The first electronic origin of THDC-d_8 is however blue-shifted by 130.1 cm^{-1} relative to the first electronic origin of THDC-d_0 because of the changes in zero point vibrational energies in the ground and excited states upon deuteration. Listed in Table 2 are: the frequencies of the observed peaks in the spectra of THDC-d_0 and THDC-d_8, the isotope effects in THDC-d_8, and the proposed assignments of the observed peaks. The isotope effects, IE, were calculated as the percentage decrease of the frequencies (relative to the first observed peak at 36956.3 cm^{-1}) of the observed peaks in the spectrum of THDC-d_8 with respect to the frequencies of the corresponding peaks in the spectrum of THDC-d_0. As seen in Table 3, the peak at 37147.9 cm^{-1} has a negligible isotope effect of 0.4%, suggesting that the peak at 37147.9 cm^{-1} is an electronic origin of another THDC conformer [16]. All other peaks have isotope effects of at least −3%. These observations indicate that only two THDC conformers with electronic origins at 36956.3 and 37147.9 cm^{-1} are present

Table 2 Assignment of the observed peaks in the R2PI spectra of THDC-d_0 and THDC-d_8

THDC-d_0		THDC-d_8			Assignment
Transition energy (cm^{-1})	Vibrational energy υ_{d_0} (cm^{-1})	Transition energy (cm^{-1})	Vibrational energy υ_{d_8} (cm^{-1})	Isotope effect (%)	
36956.3	0.0	37086.4	0.0		$S_1 \leftarrow S_0$ origin of the TB conformer
36984.8	28.5	37113.3	26.9	−5.6	v_1
37012.7	56.4	37139.4	53.0	−6.0	$2v_1$
37039.7	83.4	37164.9	78.5	−5.9	$3v_1$
37056.3	100.0	37183.2	96.8	−3.1	$S_2 \leftarrow S_0$ origin of the TB conformer
37065.7	109.4	37189.3	102.9	−5.9	$4v_1$
37070.7	114.4	37197.3	110.9	−3.1	v_2 or v_3
37100.1	143.8	37225.4	139.0	−3.3	v_2 (or v_3)+ v_1
37132.6	176.3	37257.4	171.0	−3.0	v_5
37147.9	191.6	37278.7	192.3	0.4	$S_1 \leftarrow S_0$ origin of the C conformer

Table 3 Assignment of the observed bands in the R2PI spectrum of THDC-d_4

Transition energy (cm^{-1})	Vibrational energy υ_{d_4} (cm^{-1})	Assignment
36993.2	0.0	$S_1 \leftarrow S_0$ origin ($d_0^* - d_4$), TB conformer
37021.6	28.4	v_1
37049.2	56.0	$2v_1$
37076.1	82.9	$3v_1$
37102.4	109.2	$4v_1$
37151.4	158.2	$S_2 \leftarrow S_0$ origin ($d_4^* - d_0$), TB conformer
37154.6	161.4	$S_1 \leftarrow S_0$ origin ($d_0^* - d_4$), C conformer
37167.2	174.0	
37169.3	176.1	
37181.3	188.1	
37187.0	193.8	
37196.3	203.1	
37205.0	211.8	
37217.6	224.4	
37224.6	231.4	
37286.7	293.5	$S_2 \leftarrow S_0$ origin ($d_4^* - d_0$), C conformer

in the gas phase. The two electronic origins can be assigned by comparison with the previously analyzed electronic spectra of allylbenzene [13] and alkylbenzenes [17]. The electronic origins of the compact gauche conformers of alkylbenzenes and allylbenzene (in which the substituent group points toward the aromatic chromophores) are red-shifted relative to the electronic origins of the anti conformers. The first electronic origin at 36956.3 cm^{-1} is thus assigned to the electronic origin of the TB conformer (in which the two aromatic chromophores point toward one another), and the second electronic origin at 37147.9 cm^{-1} is assigned to the origin of the C conformer.

The relative population of conformers can be estimated by integrating the areas under the vibronic peaks of each conformer in the electronic origin region of supersonic jet electronic spectrum [18, 19]. The relative abundance of the TB and C conformers was estimated by integrating the area under the origin peak of the C conformer, and the areas under the whole vibronic envelope of the TB conformer in the origin region of the R2PI spectrum [19]. The estimated TB:C population ratio is 9.1:1. Hence, 90% of THDC exists in the TB conformation in the gas phase; the C conformer constitutes the remaining 10%. The Boltzmann distribution law was then used to estimate their relative energy, $\Delta E = E_C - E_{TB}$. The statistical weight of 2 for the TB conformer, and the pre-expansion temperature of 413 K (140 °C) were used in the calculations [19]. The estimated value of ΔE is 5.20 kJ/mol. The estimated value of ΔE is very close to the MP2/6-31+G(d)//HF/6-31+G(d) calculated relative energy of 5.84 kJ/mol (Table 1). The latter is about half of the MP2/6-31+G(d)//MP2/6-31+G(d) calculated relative energy of 11.76 kJ/mol. The failure of the MP2/6-31+G(d)//MP2/6-31+G(d) calculations to reproduce the experimental relative energy can be attributed to the overestimation of conjugation by the MP2 method [14]. It was concluded from NMR experiments in CD_2Cl_2 solution that THDC exists as a mixture of the TB (88%) and C (12%) conformers [3]. Therefore, the TB conformer predominates in the gas and liquid phases. The higher stability of the TB conformer can be attributed to non-bonded intramolecular dispersive interactions between the π electron clouds of the aromatic rings [13].

Listed in Tables 2 and 3 are the proposed assignments of the observed peaks in the R2PI spectra of THDC isotopomers. Assignments of vibrational modes was performed by comparison with the HF/6-31+G(d) and B3LYP/6-31+G(d) calculated vibrational modes. THDC has 90 normal modes; listed in Table 4 are the HF/6-31+G(d) and B3LYP/6-31+G(d) calculated frequencies and approximate descriptions of the five lowest frequency vibrational modes of the TB conformer in the ground state. A progression with a fundamental frequency of 28.5 cm^{-1} is built off of the electronic origin of the TB conformer. The first two calculated lowest frequency modes differ significantly in frequency (47 vs. 95 cm^{-1} at the HF/6-31+G(d) level, 42 vs. 88 cm^{-1} at the B3LYP/6-31+G(d) level). Therefore, the plausible assignment for the observed 28.5 cm^{-1} fundamental is to the lowest frequency mode, labeled v_1 in Table 4. This mode involves symmetric flapping of the two aromatic rings. The appearance of a progression in a flapping mode with the first and second members of the progression being more intense than the electronic origin indicates geometrical changes in the excited state of the TB conformer. The geometrical changes are along the flapping mode of the two aromatic rings (i.e., the values of the four $\mathrm{C_{sp^2}{-}C_{sp^3}{-}C_{sp^3}}$ angles would change upon excitation to the S_1 state). The change in the values of the four $\mathrm{C_{sp^2}{-}C_{sp^3}{-}C_{sp^3}}$ angles is the most likely reason for the observation of unstructured fluorescence of THDC in solution [5]. This provides additional evidence for the predomination of the TB conformer in both liquid and gas phases. More theoretical work is needed to determine the exact changes in the values of the four $\mathrm{C_{sp^2}{-}C_{sp^3}{-}C_{sp^3}}$ angles.

The peak at 114.4 cm^{-1} can be assigned to mode v_2 or v_3 based on the similar values of the observed and calculated frequencies. This mode appears in combination with mode v_1 at 143.8 cm^{-1}. Similarly, the very weak peak at 176.3 cm^{-1} can be assigned to mode v_5. The peak at 100.0 cm^{-1} is not associated with an overtone or combination peak; hence, it is tentatively assigned to the $\mathrm{S}_2 \leftarrow \mathrm{S}_0$ origin of the TB conformer.

The spectrum of THDC-d_4 presented in Fig. 3b was recorded for the purpose of obtaining the experimental exciton splitting of the C conformer, and confirming the tentative assignment of the $\mathrm{S}_2 \leftarrow \mathrm{S}_0$ transition of the TB conformer. Listed in Table 3 are the frequencies of the observed spectral features of THDC-d_4, and their proposed assignments. A four-membered progression with a fundamental frequency of 28.4 cm^{-1} also appears in the spectrum of THDC-d_4. As shown in Fig. 3b, four localized electronic origins have been identified in the spectrum of THDC-d_4. The four origins are associated with the localized excitations of the deuterated ($d_4^* - d_0$) and undeuterated ($d_0^* - d_4$) aromatic rings of the C and TB conformers. The $\mathrm{S}_2 \leftarrow \mathrm{S}_0$ transitions are localized on the deuterated aromatic rings ($d_4^* - d_0$); while the $\mathrm{S}_1 \leftarrow \mathrm{S}_0$ transitions are localized on the undeuterated aromatic rings. The zeroth-order excited states are no longer degenerate in THDC-d_4. Thus, there exists a possibility of resonance and/or near resonance interactions between the vibronic states that are more or less localized on the undeuterated ring of THDC-d_4 with those localized on the deuterated ring, and vice versa. This, together with the lower symmetry of THDC-d_4 may lead to a complex vibronic pattern in the spectrum of THDC-d_4.

Exciton couplings

The method outlined by Baum and McClure [9] was used to estimate the exciton splittings, $2V_{00}$, in the electronic spectrum of THDC using the observed 0_0^0 transition energies of THDC-d_0 and THDC-d_8 (Table 2), and the localized 0_0^0 transition energies of THDC-d_4 (Table 3). The estimated values of $2\mathrm{V}_{00}$ in the TB and C conformers are 101.9 and 14.7 cm^{-1}, respectively. These experimentally based results confirm the assignment of the band at 100.0 cm^{-1} in the spectrum of THDC-d_0 to the $\mathrm{S}_2 \leftarrow \mathrm{S}_0$ origin of the TB conformer, and that the $\mathrm{S}_2 \leftarrow \mathrm{S}_0$ origin of the C conformer is forbidden in the symmetric THDC-d_0 and THDC-d_8.

The electronic coupling energy, V, was then estimated by dividing V_{00} with the Franck–Condon factor, $\mathrm{FC}_{0\text{–}0}$, for the 0_0^0 transition of *o*-xylene (the presumed monomer of THDC) [9]. A $\mathrm{FC}_{0\text{–}0}$ of 0.25 was estimated by dividing the

Table 4 Summary of the HF/6-31+G(d) and B3LYP/6-31+G(d) calculated lowest frequency vibrational modes of the TB conformer

Mode	Freq. (cm^{-1})		Approximate description
	HF	B3LYP	
v_1	47	42	Symmetric flapping of aromatic rings
v_2	95	88	Symmetric torsion about $\mathrm{C_{sp^3}{-}C_{sp^2}}$ bonds
v_3	139	127	Asymmetric torsion about $\mathrm{C_{sp^3}{-}C_{sp^3}}$ bonds + asymmetric flapping of aromatic rings
v_4	149	139	Asymmetric torsion about $\mathrm{C_{sp^3}{-}C_{sp^2}}$ bonds
v_5	178	163	$\mathrm{-CH_2{-}CH_2{-}}$ bridge deformation

Table 5 CIS/6-31+G(d)//HF/6-31+G(d) calculated vertical $S_1 \leftarrow S_0$ and $S_2 \leftarrow S_0$ excitation energies (E_1 and E_2, cm^{-1}) with their oscillator strengths (f_1 and f_2), and the symmetries of the excited states of the TB and C conformers

Conformer	$S_1 \leftarrow S_0$			$S_2 \leftarrow S_0$			$E_2 - E_1$
	E_1	f_1	Symmetry	E_2	f_2	Symmetry	
TB	48440	0.0051	B	48807	0.0016	A	367
C	48713	0.0042	B_u	48772	0.0000	A_g	59

area under the 0_0^0 band to that under the whole L_b band of the room temperature absorption spectrum of *o*-xylene. Hence, the experimental values of V are 200.0 and 29.4 cm^{-1} for the TB and C conformers, respectively.

The supramolecular model of dimers that is composed of two identical chromophores takes into account all kinds of through-space and through-bond exciton interactions [6–8]. According to the supramolecular model, the electronic coupling energy, V, is equal to the half of the energy gap between the calculated $S_1 \leftarrow S_0$ and $S_2 \leftarrow S_0$ vertical excitation energies. The intensities of the $S_1 \leftarrow S_0$ and $S_2 \leftarrow S_0$ transitions are proportional to their oscillator strengths. As seen in Table 5, the S_1 and S_2 states of the C conformer have B_u and A_g symmetries, respectively; hence, the $S_2 \leftarrow S_0$ transition of the C conformer is predicted to be one-photon forbidden. The calculated energy gap between the two states is 59 cm^{-1}. On the other hand, the S_1 and S_2 states of the TB conformer have B and A symmetries, respectively. Both $S_1 \leftarrow S_0$ and $S_2 \leftarrow S_0$ transitions of the TB conformer are predicted to be allowed, the former being ca. three times more intense than the latter. The calculated energy gap between the S_2 and S_1 states of the TB conformer is 367 cm^{-1}. Therefore, at the CIS/6-31+G(d)//HF/6-31+G(d) level of theory, the electronic coupling energies, V, of the C and TB conformers are 29.5 and 183.5 cm^{-1}, respectively. These values are very close to the experimentally estimated coupling energies of 29.4 and 200 cm^{-1} for the C and TB conformers, respectively. However, it should be noted that the results of the supramolecular model are very sensitive to the level of theory employed [6, 8]; hence, the good agreement with the experimentally estimated results obtained in this work is accidental.

The large difference in the exciton coupling energies of the two conformers is attributed to through-space interactions. Effective orbital overlap of the two aromatic rings of the compact TB conformer enhances through-space interactions of the two aromatic chromophores. Through-bond interactions generally depend on the number of σ bonds between the chromophores, and the energy gap between the aromatic ring localized $\pi\pi^*$ states and aliphatic bridge localized $\sigma\sigma^*$ states [7]. These parameters are expected to be similar in the two THDC conformers. For instance, the values of the through-bond coupling that influences the length of the central $C_{sp^3}-C_{sp^3}$ of 1,2-diphenylethane is calculated to be equal to 0.3 eV for both gauche and anti conformers of 1,2-diphenylethane [20].

Conclusions

In the gas phase, THDC predominantly exists (about 90%) in the twist-boat (TB) conformation; the chair (C) conformer constitutes the remaining 10%. Most of the vibronic peaks in the spectrum of THDC are associated with the symmetric flapping of the aromatic rings of the TB conformer. The $S_2 \leftarrow S_0$ transition of the C conformer is forbidden. The observed exciton splitting of the TB conformer is 100 cm^{-1}. The estimated exciton splittings in the spectra of the C and TB conformers are 14.7 and 101.9 cm^{-1}, respectively. The supramolecular model of bichromophores with identical chromophores at the CIS/6-31+G(d) level of theory predicted electronic coupling energies that are very close to the experimental coupling energies.

Acknowledgment The author is grateful to Dr. John R. Cable, Bowling Green State University, Ohio, for his generous support of this work.

References

1. Domiano P, Cozzini P, Claramunt RM, Lavandera JL, Sanz D, Elguero J (1992) J Chem Soc Perkin Trans 2 11:1609
2. Montecalvo D, St-Jacques M, Wasylishen R (1973) J Am Chem Soc 95:2023
3. Jimeno ML, Alkorta I, Elguero J, Anderson JE, Claramunt RM, Lavanderac JL (1998) New J Chem 22:1079
4. Allinger NL, Sprague JT (1975) Tetrahedron 31:21
5. Longworth JW, Bovey FA (1966) Biopolymers 4:1115
6. Clayton AHA, Scholes GD, Ghiggino KP, Paddon-Row MN (1996) J Phys Chem 100:10912
7. Scholes GD (2003) Annu Rev Phys Chem 54:57
8. Curutchet C, Mennucci B (2005) J Am Chem Soc 127:16733
9. Baum JC, McClure DS (1980) J Am Chem Soc 102:720
10. Boudjouk P, Sooriyakumaran R, Byung HH (1986) J Org Chem 51:2818
11. Finley JP, Cable JR (1993) J Phys Chem 97:4595
12. Frisch MJ, Trucks GW, Schlegel HB, Scuseria GE, Robb MA, Cheeseman JR, Montgomery JAJR, Vreven T, Kudin KN, Burant JC, Millam JM, Iyengar SS, Tomasi J, Barone V, Mennucci B, Cossi M, Scalmani G, Rega N, Petersson GA, Nakatsuji H, Hada M, Ehara M, Toyota K, Fukuda R, Hasegawa J, Ishida M,

Nakajima T, Honda Y, Kitao O, Nakai H, Klene M, Li X, Knox JE, Hratchian HP, Cross JB, Adamo C, Jaramillo J, Gomperts R, Stratmann RE, Yazyev O, Austin AJ, Cammi R, Pomelli C, Ochterski JW, Ayala PY, Morokuma K, Voth GA, Salvador P, Dannenberg JJ, Zakrzewski VG, Dapprich S, Daniels AD, Strain MC, Farkas O, Malick DK, Rabuck AD, Raghavachari K, Foresman JB, Ortiz JV, Cui Q, Baboul AG, Clifford S, Cioslowski J, Stefanov BB, Liu G, Liashenko A, Piskorz P, Komaromi I, Martin RL, Fox DJ, Keith T, Al-Laham MA, Peng CY, Nanayakkara A, Challacombe M, Gill PMW, Johnson B, Chen W, Wong MW, Gonzalez C, Pople JA (2003) Gaussian 03, Revision B.03. Gaussian, Inc, Wallingford, CT

13. Panja SS, Chakraborty T (2003) J Chem Phys 118:6200
14. Page CS, Merchan M, Serrano-Andres L, Olivucci M (1999) J Phys Chem A 103:9864
15. Smith GD, Ayyagari C, Jaffe RL, Pekny M, Bernarbo A (1998) J Phys Chem A 102:4694
16. Im HS, Bernstein ER, Secor HV, Seeman JI (1991) J Am Chem Soc 113:4422
17. Hopkins JB, Powers DE, Smalley RE (1980) J Chem Phys 72:5039
18. Al-Saadi AA, Wagner M, Laane J (2006) J Phys Chem A 110:12292
19. Manea VP, Wilson KJ, Cable JR (1997) J Am Chem Soc 119:2033
20. Baldridge KK, Battersby TR, VernonClark R, Siegel JS (1997) J Am Chem Soc 119:7048